Investigation of Structural, Morphological, Electrical & Magneto-transport Properties of $Nd_{0.5}Ba_{0.5}MnO_3$ Nanoparticles

[1]Jessica R.Chocha, [2]Jayant A. Bhalodia,
[1] Assistant Professor, Department of Physics, Bahauddin Science College, Junagadh, Gujarat, India.
[2] Associate Professor, Department of Physics, Saurashtra University, Rajkot, Gujarat, India.
Email – [1] jessicaphysics@gmail.com [2] jabrajkot@rediffmail.com

Abstract: *This study reports on the Ba-doped $NdMnO_3$ nanocrystalline CMR manganites having the perovskite structure prepared citrate pyrolysis method. To obtain the $Nd_{0.5}Ba_{0.5}MnO_3$(NBMO) nanoprticles, calcination of precursor was carried out at the temperature of 200 ºC, 300 ºC, 600 ºC & 900 ºC, for very short time duration ~ 2 h. The synthesized NBMO were characterized by TG/DTA, XRD, FT-IR, TEM, AFM and electrical magneto-transport properties. Thermal analysis shows no more weight loss in the NBMO compounds prepared at 200 ºC. Structural characterization shows that the prepared compounds consists of orthorhombic phase without impurities in the sample calcined at 900 ºC, 2h and with crystalline size of ~ 25 - 35 nm as determined by scherrer's formula. The Mn-O-Mn bond was identified by the measurements of Infrared IR transmission spectra. The resistivity (ρ) suppresses and T_{MI} values increases with increasing magnetic field for NBMO calcined at 900 ºC and shows positive MR % values. Detail discussion will be in the light of calcination temperature and magnetic field variation effect on the structure, particle size, purity and resistivity of the compound in this communication.*

Key Words: *CMR, Perovskite, NBMO, Nanoparicles. Synthesis,*

1. INTRODUCTION:

The discovery of colossal magneto-resistance (CMR) in manganese oxides has renewed the interest in these materials, where a high correlation between structural, transport, and magnetic properties is found. More recently, their bulk polycrystalline forms were found to exhibit a low-field sensitive and wide temperature-independent extrinsic CMR effect, which is favourable to potential applications [1-4]. The perovskite manganites $A_{1-x}B_xMnO_3$ where A is a trivalent lanthanide cation (e.g. La, Nd, Pr...) and B is a divalent cation (e.g. Ca, Sr, Ba...) have recently attracted much attention because of their technical applications. This phenomenon is attributed to the grain boundaries especially for the granular manganites. Magnetic nanoparticles with smaller grain sizes exhibit richer electronic and magnetic properties arising from structural and magnetic disorders in the grain surfaces. Recently, modification of the properties of nano-sized perovskites has aroused much interest [5,6]. The physical properties of CMR compounds are influenced by several parameters [7]. The chemical composition mainly affects the magnetic behavior and the magnetic and electrical transition temperatures. The synthesizing methods are very important to obtain the polycrystalline with special microstructure. In general, these oxides are synthesized at high temperatures using a standard ceramic technique, and hence the microstructure is difficult to be governed. Chemical preparation methods called "soft chemistry processing" such as sol–gel [8, 9] and co-precipitation methods [10 - 13] have been introduced to synthesize the CMR oxides. All these methods maintain the metal precursors in a highly dispersed state, and hence favor more homogenous powders at relatively low temperatures. Most of the studies done on Ba-substituted compounds are lanthanum barium manganites [14]. We successfully overcome this barrier by utilizing a simple, versatile and easy chemical process. Only a few attempts have been tried because the NBMO crystals have three different metals and thus homogeneous stoichiometric composition is not easily obtaining through citrate pyrolysis process. The method is fast, simple and cost effective, which is a promising synthesis route for the preparation of metal oxide and complex oxide nano-particles. In this paper, we have synthesized a barium concentration substituted neodymium compound $Nd_{1-x}Ba_xMnO_3$ and the results of such an investigation are presented here.

2. METHOD:

The $Nd_{1-x}Ba_xMnO_3$ (x = 0.5) compound were prepared using the citrate pyrolysis technique. High purity neodymium oxide (99.9%), barium carbonate (99.9%), manganese dioxide (99.9 %), citric acid (99.9 %,), nitric acid and ethylene glycol were used as starting materials. In typical procedure, Nd_2O_3, $BaCO_3$ & MnO_2 were mixed thoroughly in agate mortar 5-10 minutes and then the resulting precursor was dissolved in a nitric acid (HNO_3) solution at about 80 ºC. After 0.3 mole citric acid and 0.1 mole of ethylene glycol were dissolved in de-ionized water and then mixed with the above nitric acid (HNO_3) solution, under continuous stirring, the resulting solution was heated at 80 – 90 ºC until each turned into brown colored gel. Then dark brown resin was obtained from the brown gel by drying at 150 ºC for 1440 minutes in an oven. Finally, the resulting resin was pulverized and then calcined at various temperatures to optimize synthetic condition of the NBMO nanoparticle.

2.1 INSTRUMENTATION:

The TG-DTA measurements were performed on a LINSEIS STA PT-1600 analyzer. The precursor was heated in air (20 - 900° C, 10° C/min) in ceramic crucible, which also served as the reference. The infrared spectra were recorded as KBr pellets on a Nicolet-6700 Thermo Scientific FTIR spectrometer. FTIR spectrometer on a sample of hardened $Nd_{0.5}Ba_{0.5}MnO_3$ gel precursor obtained by drying the formulated at 150º C. Survey scans for determining the effects of temperature on the evolution of crystalline NBMO perovskite were investigated by θ-2θ X-ray powder diffraction (XRD) using a Philips Netherland Xpert model diffractometer. Samples were ground to a fine powder spred on a glass plate. X-ray diffraction patterns were collected in the range 20 – 80º with 0.02º steps using Cu–Kα radiation. The morphologies of the calcined powders were observed using a scanning electron microscopy (SEM-Philips Netherland XL-30.

3. RESULTS:

3.1. THERMAL GRAVIMETRIC ANALYSIS (TG-DTA):

The mechanisms of the thermal decomposition of the NBMO dried gels were studied by TG/DTA analyses, under ambient conditions. The TG-DTA results of the composition $Nd_{0.5}Ba_{0.5}MnO_3$, precursors dried at 200 ºC, 2 h are shown in figure 1 respectively. The TG-profile shows 20-240 ºC, 240-260 ºC, 300-400 ºC and 700 - 800 ºC regions in all NBMO compound. This technique produces poly nuclear, metal complexes in the aqueous gel phase which would allow for strong intermolecular mixing, promote metal-oxygen metal polymerization during the pre-calcination phase, and facilitate the crystallization of NBMO at relatively low temperature. The subsequent weight loss corresponds to the sluggish decomposition of the neodymium oxy-carbonate $Nd_2O_2CO_3$ formed during the first step of the heating process. The second and most significant decomposition step (~ 700 - 800 ºC) region can be attributed to the pyrolysis of organic compounds and the degradation of intermediate species formed during the gelation process as shown in figure. This observation is corroborated by a prominent exothermic in the DTA curve. The broad endothermic (~ 344 - 380 ºC) can be attributed to the beginning of ordering and crystallization processes. Since the structure of the gel complexes has not been investigated, a more detailed interpretation of the decomposition mechanism is difficult. No remarkable weight loss is observed after ~ 860 ºC indicating the formation of an oxide with a definite composition.

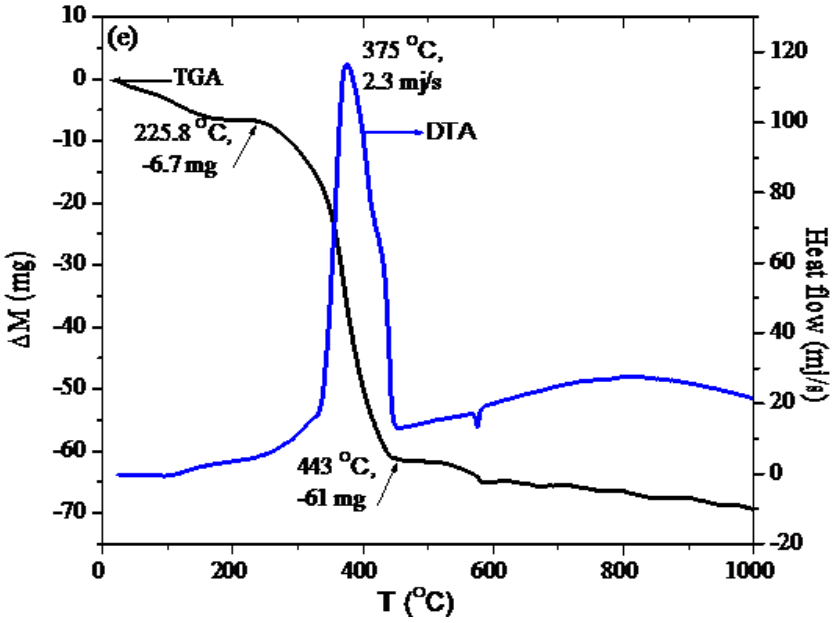

Figure 1: TG-DTA profile for $Nd_{0.5}Ba_{0.5}MnO_3$ composition dried at 200 °C, 2 h.

3.2. FOURIER TRANSMISSION INFRARED SPECTROSCOPY FT-IR):

Figure 2 shows the FT-IR spectra for the dried powders of $Nd_{0.5}Ba_{0.5}MnO_3$ compound at 200 ºC, for 2 h. In figure the absorption peaks around 1650 cm^{-1} and 2350 cm^{-1} are of carrier $KBr(H_2O)_n$ and CO_2, respectively [15]. In the infrared absorption spectra of inorganic carbonate compounds are very distinctive in all NBMO compound. The C=O and C-N stretching bands sharp peak at ~ 1542 cm^{-1} and ~1356 cm^{-1} are present in all the NBMO compound. According to literature results, $BaCO_3$ presents bands at 1750, 1460, 1060, 860 and 700 cm^{-1}. The absorption peaks around 600 cm^{-1} and 434 cm^{-1} should belong to stretching and bending of the internal phonon modes of MnO_6 octahedral. The stretching mode is related to the change of Mn-O-Mn bond length and the bending mode involves the change of Mn-O-Mn bond angle. All of the band positions are somewhat dependent on the hydration state of the sample. Alcohols are compounds which contain the hydroxyl (-OH) group. These compounds are classified as primary, secondary or tertiary according to the number of other carbon atoms attached to the oxygen bound carbon.

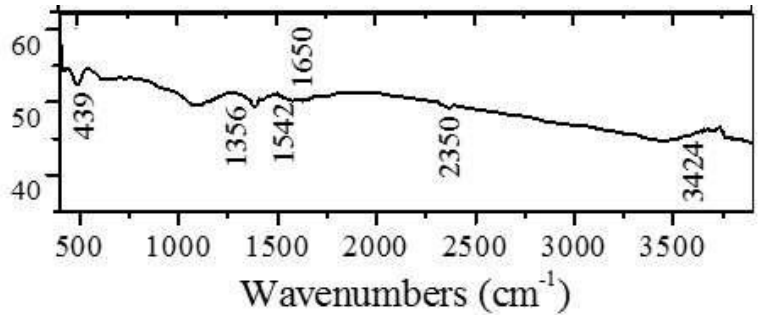

Figure 2: FT-IR spectra for $Nd_{0.5}Ba_{0.5}MnO_3$ composition dried at 200 °C, 2 h.

3.3. X-ray DIFFRACTION (XRD):

The transformation of crystalline NBMO compositions perovskite bulk powders should, in principle, depend on calcination temperature. The XRD results of the prepared NBMO compound at 200 ºC, 300 ºC, 600 ºC, and 900 ºC for 2 h are shown in figure 3. By increasing the calcination temperature from 300 ºC to 600 ºC, the crystalline phase produces but still extra minor peaks were found in the NBMO compound. The figure shows neodymium-barium manganite to be the only crystalline single phase and not impurity phase in all the NBMO compositions calcined at 900 ºC for 2 h. The diffraction peaks in all the NBMO samples show sharper profiles resulting from the combination of crystallization/ordering process and gradual grain growth, which are in accordance to the orthorhombic symmetry reduction of this perovskite with the same space group Pnma No. 62.

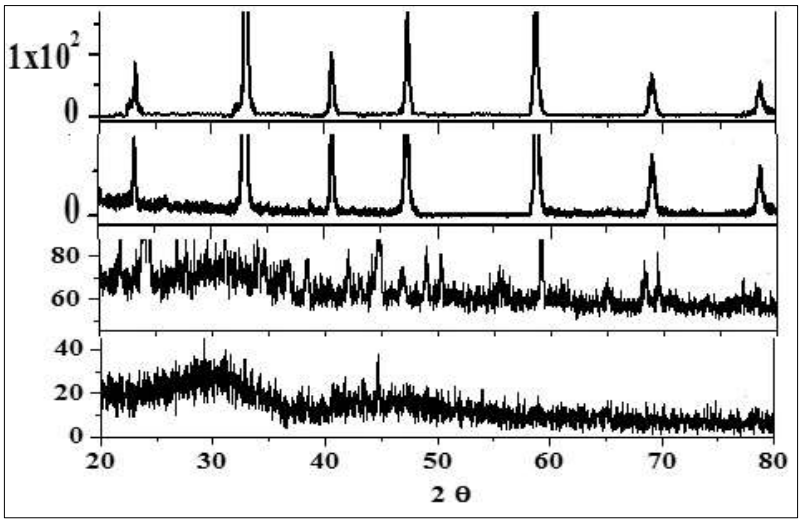

Figure 3: XRD patterns of $Nd_{0.5}Ba_{0.5}MnO_3$ samples calcined at 200 ºC, 300 ºC, 600 ºC & 900 ºC for 2 h.

The room temperature lattice parameters slightly change with increasing Ba concentration value from x =0.5 in the NBMO compound calcined at 900 °C as shown in table 1. The peaks were broad indicating the fineness of the powders. Calcination at higher temperatures did not change the peak position much, but the peaks became sharper and higher in intensity indicating an increase in crystallite size. The crystallite sizes of the synthesized samples were determined from XRD line broadening of the largest intensity for a single peak at 2θ around at 32 ºC using the Debye Scherrer's equation.

$$D = \frac{k\lambda}{\beta \cos\theta}$$

Where k is the particle shape factor (= 0.9 considering the circular shape of the nanoparticles). λ = 1.5405 Å is the wavelength of CuKα radiation, β is the full width at half maximum of the XRD (200) peak, and θ is the diffraction angle of the peak. The obtained crystallite sizes as a function of the Ba-concentration for the calcined NBMO at 1000 °C for 2 h are listed in Table 1. The crystalline sizes were found to be around 25 for NBMO (x =0.5) compound calcined at 900 ºC, 2 h, respectively.

3.4. TRANSMISSON ELECTRON MICROSCOPY (TEM):

For NBMO compositions particle sizes were also confirmed by transmission electron microscope (TEM) measurements. The typical transmission electron microscope images of the NBMO sample are shown in figure 4 Closer inspection of the TEM shows that the nanoparticles of the NBMO all compositions studied have nearly sphere like elementary shape and the particles were arranged in chains. Analysis of the particle diameters reveals that the particle size was in the nanometer range for each NBMO composition. The present results indicate that the application

of surfactant not only improves the stoichiometry of the nanoparticles but also narrow the particle size distributions. The average particle size of NBMO (x = 0.5) compositions was in the range around. The TEM images indicate the highly crystalline nature of the heat treated samples at 900 ºC for lower time duration (2 h). It is clearly seen from the TEM images that the average particle size decreases with increasing Ba concentration. This is in the best agreement with the results estimated from the X-ray diffraction for the different NBMO compositions which can be seen from the table 1.

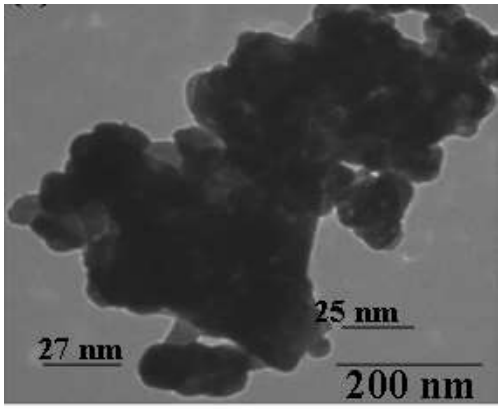

Figure 4: TEM images of $Nd_{0.5}Ba_{0.5}MnO_3$ sintered at 900 ºC, for 2 h.

3.5. ATOMIC FORCE MICRSCOPY (AFM):

The surface morphology of the different NBMO compositions has been studied by contact mode atomic force microscope (AFM). Atomic force microscopy (AFM) of the different NBMO compositions in pellet forms carried out are shown in figure 5. The AFM two dimensional (2D) images of NBMO (x = 0.5) sintered pellets at 900 ºC, 2 h, show uniformly clear grain formation with a spherical shape having a wide distribution. Analysis of the AFM images reveals that crystalline blocks have a narrow size distribution with mean grain size in nanometer range. The average grain sizes and surface roughness values are also presented in table 1. The AFM three dimension (3D) view of NBMO (x = 0.5) samples sintered at 900 °C, 2 h, is shown in figure. The 3D images of different NBMO compositions is in 1.0 μm ×1.0 μm scale and its Z- scale is in nanometer range. The 3D view of the NBMO samples indicates clearly the grain growth and notes the grain boundaries between these grains. The surface roughness diagram of the different NBMO compositions are shown in figure 5. The RMS values decease with decreasing the Ba concentration values. The AFM results also confirm that grain size decreases with increasing Ba concentration and it was also in good agreement with XRD and TEM results.

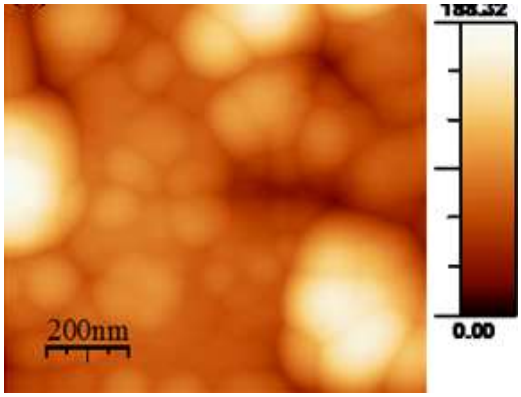

Figure 5: AFM 2D images of $Nd_{0.5}Ba_{0.5}MnO_3$ sintered at 900 ºC, for 2 h.

3.6. ELECTRICAL RESISTIVITY:

The temperature dependence of the electrical resistivity ρ(T) measured in absence and different presence magnetic fields (1 T, 5 T, 9 T & 14 T) are shown in figure 6. Figure shows temperature dependence resistivity in the different magnetic fields (0 T, 1 T, 5 T, 9 T & 14 T) for the NBMO (x = 0.5) samples sintered at 900 ºC, 2 h. In the absence of magnetic field, all the NBMO compound have a maximum value in the temperature dependence of the resistivity near T_c shown in figure. For NBMO, x = 0.5, the resistivity can be divided into different regions between 2 and 350 K which correlates well with the two magnetic phase transitions. With decreasing temperature the resistivity increases monotonically down to 83 K, characteristic of an insulator/semiconductor ($d\rho/dt < 0$). The resistivity reaches a peak at T = 83 K, then decreases rapidly as temperature is decreased to ~ 32 K. This metallic behaviour is induced by the ferromagnetic ordering that drastically enhances the electron hopping rate for Mn^{+3}, Mn^{+4} which strongly

depends on the relative orientation of the Mn ions. The low temperature below around 32 K increase in resistivity can be due to the tunnelling states resulting from the grain boundaries. $Nd_{0.5}Ba_{0.5}MnO_3$ sample with their maxima near transitions increase up to ~ 100 K. The maximum zero field resistivity value is 3726.2151 Ω cm for NBMO. The metal insulator transition temperatures at zero field (T_{IM}) values are indicated in table 2.

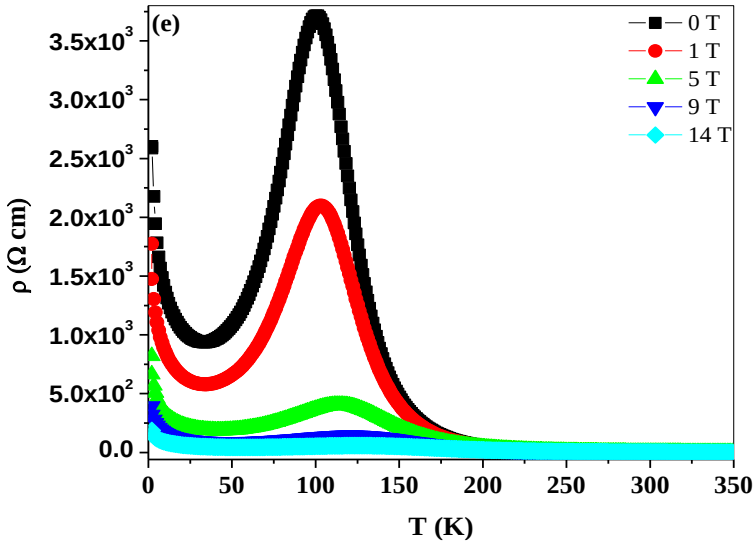

Figure 6: The temperature dependence resistivity of the $Nd_{0.5}Ba_{0.5}MnO_3$ sample sintered at 900 ºC, 2 h, with different magnetic fields.

3.6. MAGNETO-RESISTANCE (MR %):

The magneto-resistance dependence of the samples sintered at 900 °C, 2 h, $Nd_{0.5}Ba_{0.5}MnO_3$ is shown in figure 7, for different magnetic fields. The percentage of magneto-resistance is defined as,

$$MR = \frac{\rho\,(H = 0) - \rho\,(H)}{\rho\,(H = 0)} \times 100\ \%$$

where, ρ(H = 0) is the resistivity without magnetic field and ρ(H) is the resistivity in a field as a function of temperature.

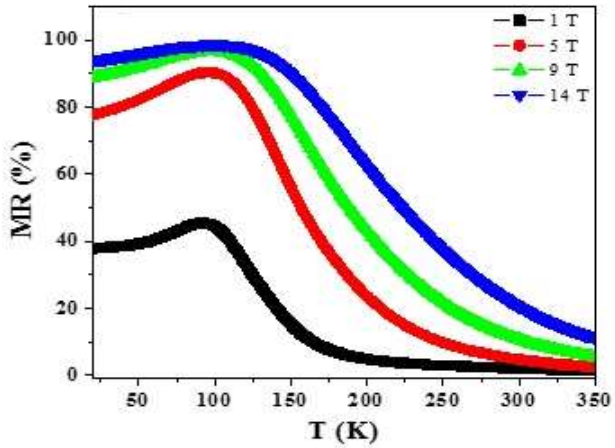

Figure 7: The temperature dependence magneto-resistance (MR) curves of $Nd_{0.5}Ba_{0.5}MnO_3$ sintered at 900 °C, 2 h.

The MR values at 1T, 5 T, 9 T & 14 T fields for all the NBMO samples are shown in table 2. Furthermore, one can see a larger MR values, increases with magnetic fields, persists over the temperature range from 83 - 112 K, the maximum MR appears at ~ 100 K, close to the paramagnetic-to-ferromagnetic transition. For MR 99 % for x = 0.5 NBMO compound near the temperature about 100 K, magnetic field at 14 T. The CMR effect has a peak wise characteristic over a narrow temperature region around the phase transition temperature as found for NBMO sample. As reported [16], the CMR values of polycrystalline materials were noticeably higher than expected for the double exchange model in the temperature range below the peak region. They attributed the higher values to a grain boundary effect and this description probably applies to the CMR behaviour of these samples. The dependence of variation of the magneto-resistance (MR) on the magnetic fields varying from 0 - 14 T at different temperatures has also been

studied for NBMO sample sintered at 900 °C, 2 h. In this set, the magnetic field was applied perpendicular to the current direction.

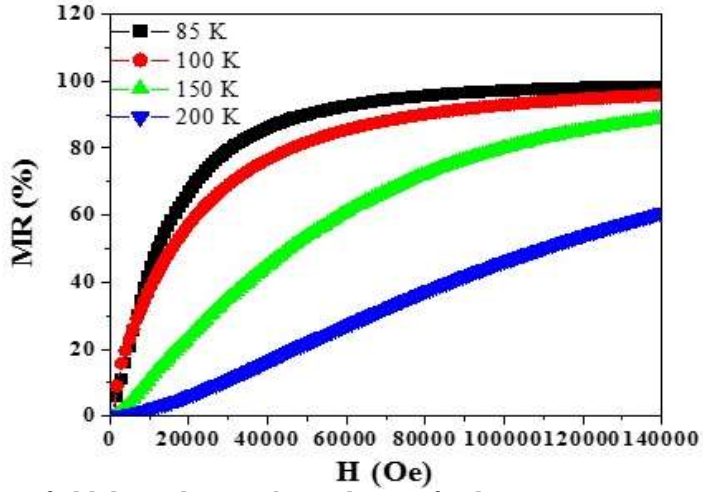

Figure 8: Magnetic field dependent isothermal MR of $Nd_{0.5}Ba_{0.5}MnO_3$ sintered at 900 C, 2 h.

This MR behaviour for x = 0.5 at different temperatures: 85 K, 100 K, 150 K & 200 K is plotted in figure 8. It is clear from the plots that the increase in MR is faster at lower temperatures than that at higher temperatures in all the NBMO sample. The important point was observed that, at 85 K (near the T_p of the NBMO), the MR values found to be higher than at the constant temperatures of 100 K, 150 K & 200 K for all NBMO, sample. Furthermore, as seen in figure 9, the rate of increase in MR with applied magnetic field is larger at low applied fields and almost MR linear with varying field. As suggested by Pignard et al [17] that such behaviour is associated with domain rotations caused by the applied field. When, one-by-one, all of domains is oriented by the increasing field and when all the electrons are parallel to the magnetic field, the scattering of polarized electrons is reduced. The low field MR (LFMR) is expected to be due to polarization of electrons in the magnetically disordered regions near the grain boundaries. The large values of the MR observed in this case at relatively low applied magnetic fields seems to be due to the presence of a large number of grain boundaries. As was explained by Wang *et al.* [18], when the grain size coincides with the ferromagnetic domain size, the domain walls will coincide with the grain boundaries.

Table 1:

Tolerance factor	**Cell parameters**	**Unit Cell voume**	**X-ray density**	**Size various**	**Crystalline size XRD TEM AFM**			**Surface roughness**	**T_{IM}**	**T_{MR}**
0.96	a = 5.5234 b = 5.5134 c = 7.7741	236.742	1.709	0.02356	15	25	35	51	100 K	99%

Table 2:

Magnetic field (H)	**ρ_0 (Ω cm)**	**$\rho_2 T^2$(Ω cm K^{-2})**	**$\rho_{4.5}T^{4.5}$ (Ω cm $K^{-4.5}$)**	**$\rho = \rho 0 + \rho_2 T^2 + \rho_{4.5}T^{4.5}$**
x = 0.5				
0 T	3×10^2	2×10^2	7.3×10^1	1.2×10^5
1 T	2×10^2	1.5×10^2	4.5×10^1	9×10^4
5 T	8.5×10^1	9×10^1	4×10^1	2×10^4
9 T	4×101	1.8×10^1	2×10^1	8×10^3

4. CONCLUSION:

In summary, barium substituted neodymium manganites, NBMO with x = 0.5 compound was synthesized by a short time (2h) polymeric precursor. The major advantage of this method is the formation of chemically pure and crystalline perovskite at relatively lower temperature. This chemical preparation method has potential advantages over the ceramic route, not only for achieving homogeneous mixing of components on the atomic scale easily, but also for controlling the microstructure effectively. The IR data indicate two internal phonon modes, i.e., the stretching and

bending modes of the MnO_6 octahedra, were observed in NBMO different compositions calcined at 200 °C, 2 h. Powder X-ray diffraction results do not show impurity phases in all the NBMO compositions calcined at 900 °C. XRD also indicates that all the NBMO compositions calcined at 900 °C could be indexed with an orthorhombic structure and all are of nanocrystalline in nature with crystallite sizes in the range about 25 -35 nm. The grain sizes measured with the transmission electron microscopy and atomic force microscopy were also found to be in nano-meter sizes with clear grain morphology in all the compositions. The roughness (RMS) values were observed increasing with increases the Ba concentration. The resistivity data of the NBMO compositions show that the resistivity decreases with the decrease of the Ba concentration due to the enhancement of the grain boundary effect. The NBMO compounds exhibit CMR related magnetic phase transitions at T_p = 100 K. The temperature dependence magneto-resistance result indicate the large MR value 99 % observed in the temperature range T < 115 K. Note that the $T_{MR} \approx T_{MI}$ suggests that the intrinsic MR is dominant in the system. The large magneto-resistance at very low temperature is probably associated with the re-entrant metal-to-insulator transition that accompanies the magnetic phase transition at T_{Nd}.

REFERENCES:

1. Jianwn Zhang, Eue-Soon Jang, H-Wan Chung, and Jin-Ho Choy *Bull Koren Chem. Soc*. vol.25, No.2 2004.
2. A. P. Ramirez, *J. Phys.: Condens. Matter* 9, 8171, 1997.
3. Hueso, L. E.; Rivas, J.; Rivadulla, F.; Lopez-Quintela, M. A. *J. Appl. Phys*. 86, 3881, 1999.
4. H. L. Ju, J. Gopalakrishnan, J. L. Peng, Qi Li, G. C. Xiong, T. Ventkatesan, and R. L. Greene, *Phys. Rev. B* 51 6143, 1995.
5. A. Urushibara, Y. Moritomo, T. Arima, A. Asamitsu, G. Kido, and Y. Tokura, *Phys. Rev. B 51*, 14, 103, 1995.
6. Leslie-Pelecky DL, Rieke RD *Chem Mater, 8*, 1773, 1996.
7. Skomski R *J Phys: Condens Matter* 15, R841, 2003.
8. Alivisatos AP *Science 271,* 933, 1996.
9. Zhu , Shen BG, Sun JR, Zhao HW, Zhou WS *Appl Phys Lett. 78*, 3863, 2001.
10. F. Gao, R.A. Lewis, X.L. Wang, S.X. Dou *J. Alloys Compd. 347*, 314, 2002.
11. C. Zener *Phys. Rev. 82*, 403, 1951.
12. P. G. de Gennes *Phys. Rev. 118*, 141, 1960.
13. R.D. Sa´nchez, J. Rivas, C. Va´zquez-Va´zquez, M.A. Lo´pez- Quintela, M.T. Cause, M. Tovar, S.B. Oseroff *Appl. Phys. Lett. 68* 134, 1996.
14. P. Dura´n, D. Gutierrez, J. Tartaj, M.A. Bana˜res, C. Moure *J. Eur. Ceram. Soc. 22,* 797–807, 2002.
15. Louca D, Egami T, Brosha E L, Roder H, and Bishop A R *Phys. Rev. B 56* R8475, 1997.
16. H. Yoshizawa, H. Kawano, Y. Tomioka, and Y. Tokura *Phys. Rev. B 52*, R193145, 1995.
17. Pignard S, Vincent H, Senateur J P, Frohlick K and Souc *J Appl. Phys. Lett.* 73, 999, 1998.
18. Wang X L, Dou S X, Liu H K, Ionescu M and Zeimetz B *Appl. Phys. Lett.* 73, 396, 1998.